Research in Astron. Astrophys. **2013** Vol. **13** No. **8**, 885–898
http://www.raa-journal.org *http://www.iop.org/journals/raa*

***R**esearch in*
***A**stronomy and*
***A**strophysics*

A multiwavelength view of the ISM in the merger remnant galaxy Fornax A

Swati Pralhadrao Deshmukh[1], Bhagorao Tukaram Tate[2], Nilkanth Dattatray Vagshette[3], Sheo Kumar Pandey[4], and Madhav Khushalrao Patil [3,†]

[1] Department of Physics, Institute of Science, Nagpur 440 008, India
[2] Department of Physics, Balbhim Arts, Science and Commerce College, Beed 431 122, India
[3] School of Physical Sciences, Swami Ramanand Teerth Marathwada University, Nanded 431 606, Maharashtra, India; *patil@iucaa.ernet.in*
[4] School of Studies in Physics & Astrophysics, Pandit Ravishankar Shukla University, Raipur 491 010, Chhattisgarh, India

Received 2012 July 18; accepted 2013 March 19

Abstract We present multi-wavelength imagery of the merger remnant galaxy NGC 1316 with an objective to study the dust content and its association with the other phases of the interstellar medium. Color-index maps as well as extinction maps derived for this galaxy reveal an intricate and complex dust morphology in NGC 1316, i.e. there is a prominent lane in the inner part, while at about 6–7 kpc it apparently takes the form of an arc-like pattern extending along the northeast direction. In addition to this, several other dust clumps and knots are also evident in this galaxy. The dust emission mapped using *Spitzer* data at 8 μm indicates even more complex morphological structures of the dust in NGC 1316. The extinction curve derived over the optical to near-IR bands closely follows the standard Galactic curve, suggesting similar properties of the dust grains. The dust content of NGC 1316, estimated from optical extinction, is $\sim 2.13\times 10^5\,M_\odot$. This is a lower limit compared to that estimated using the IRAS flux densities of $\sim$5.17$\times 10^6\,M_\odot$ and the flux densities at 24, 70 and 160 μm from MIPS $\sim$3.2$\times 10^7\,M_\odot$. High resolution *Chandra* observations of this merger remnant system have provided an unprecedented view of the complex nature exhibited by the distribution of hot gas in NGC 1316, which closely matches the morphology of ionized gas and to some extent also the dust. X-ray color–color plots for the resolved sources within the optical D_{25} extent of NGC 1316 have enabled us to separate them into different classes.

Key words: galaxies: individual (NGC 1316) — galaxies: ISM — X-rays: ISM — (ISM:) dust — extinction — galaxies: elliptical and lenticular, cD

† Corresponding author.

1 INTRODUCTION

Multiwavelength data acquired on early-type galaxies using ground-based as well as space-based telescopes have greatly enhanced our understanding regarding the origin of the multiphase interstellar medium (ISM) in this class of galaxies (Goudfrooij et al. 1994; Rampazzo et al. 2005; Patil et al. 2007; Cappellari et al. 2011; Finkelman et al. 2010, 2012). The general picture that emerges from the past studies is that either the cold/warm ISM observed in these galaxies has an external origin, accreted through merging and/or close encounters with neighboring galaxies, or is the by-product of cooling of the hot ISM that originated from stellar mass loss (Kim & Fabbiano 2003). Systematic study of these galaxies selected from different environments delineates that the relative contribution of the two competitive processes, i.e. external versus internal, does not follow a general rule regarding their origin but varies greatly among the objects. Several attempts have been made to probe the properties and origin of the ISM in early-type galaxies using spectroscopic observations studying the dynamics and chemical abundance of the gas and stars (Bertola 1987; Kormendy & Djorgovski 1989; Sarzi et al. 2006; Annibali et al. 2010). However, due to the limited spectral coverage of the study and limited knowledge about the interplay between different phases of the ISM, we could not arrive at a decisive conclusion regarding the true nature of the ISM. Therefore, a multiwavelength study of various components of the ISM in a large sample of E/S0 galaxies with dust lanes is important in investigating the nature and origin of the ISM in this class of galaxies.

Unusual optical signatures that are discernible in the form of dust-lanes, shells, tidal features, double nuclei, etc. are direct evidence indicative of merger-like events that the host galaxies might have experienced in the past (Bertola 1987; Goudfrooij et al. 2004; Patil et al. 2007). Further evidence regarding the external origin of the dust is provided by the amount of dust in such galaxies. It is found that the observed amount of dust using optical extinction measurements and IRAS flux densities is always larger by several factors than that expected from the mass loss of evolved stars (Goudfrooij et al. 2004; Dewangan et al. 1999; Patil et al. 2007). Furthermore, kinematical studies of early-type galaxies with a dust lane have revealed that the motion and orientation of the gas in many systems are decoupled from the stellar rotation, and hence provide additional evidence for their external origin (Bertola 1987; Kormendy & Djorgovski 1989; Caon et al. 2001). If the dust originated internally through the evolution of a single stellar population, then instead of forming disks, lanes, etc., it would be evenly distributed throughout the galaxy (Finkelman et al. 2012).

NGC 1316 is a peculiar S0 galaxy, with numerous tidal tails, shells and many pronounced dust patches, including the prominent dust lane oriented along its optical minor axis. In addition to dust, NGC 1316 also hosts Hα filaments, strong shells (Malin et al. 1983) and several filaments and loops of ISM (Schweizer & Seitzer 1988). All these features confirm that NGC 1316 has experienced a strong merger like episode in the past (Terlevich & Forbes 2002).

X-ray observations of this galaxy with *Einstein* (Fabbiano et al. 1992), *ROSAT* PSPC (Feigelson et al. 1995) and *Chandra* (Kim & Fabbiano 2003), and their systemic analysis, have confirmed a low luminosity AGN with 0.3–8.0 keV $L_{\rm X} \sim 5.0 \times 10^{39}$ erg s^{-1} (Kim & Fabbiano 2003), which also exhibits extended X-ray emission and has several inherent substructures. NGC 1316 is one of the nearest giant radio galaxies with a well defined core-jet-lobe structure. The lobes of this galaxy show a smooth light distribution and sharp boundaries, and the bridge of emission in NGC 1316 is found to be significantly displaced from its center, providing additional evidence for the strong merger episode (Ekers et al. 1983). Goudfrooij et al. (2001), based on the study of bright globular clusters within NGC 1316, estimated the age of this merger remnant to be $\sim$3 Gyr. Thus, NGC 1316 is a potential candidate for investigating the properties of dust and other phases of the ISM. The global parameters of NGC 1316 are given in Table 1.

In this paper, we present multicolor CCD imaging involving broadband B, V, R, I and narrow band Hα data. We mainly focus on investigating the distribution of dust, its extinction properties and compare its association with the ionized gas. We also present reanalysis of *Chandra* observations

Table 1 Global Parameters of NGC 1316

Parameter	Value
Alternate names	Fornax A; IRAS 03208–3723; PGC 012651; ESO 357–G 022 NVSS J032241–371225
RA; DEC	03:22:41.7; –37:12:30
Morphology	SAB0(s)pec / S0
Mag B_T	9.42
D_{25}	$12.0' \times 8.5'$
Redshift (z)	0.00587
Effective radius (kpc)	7.08
IR flux densities (Jy)	0.33±0.04 (12 μm); 3.07±0.03 (60 μm); 8.11±1.99 (100 μm) IRAS & 0.43±0.02 (24 μm); 5.44±0.40(70 μm); 12.61±1.78 (160 μm) MIPS

of NGC 1316. The paper is organized as follows. In Section 2 we describe the optical and X-ray observations and the data analysis process. Section 3 discusses the dust extinction properties and morphology of ionized gas. The results derived from the spatial and spectral analysis of X-ray photons, along with the discrete sources, are also discussed in this section. Section 4 discusses the origin of dust as well as its association with other phases of the ISM. Finally, we summarize our results in Section 5. We adopt an optical luminosity distance of 25 Mpc throughout this analysis.

2 OBSERVATIONS AND DATA PREPARATION

2.1 Optical and Near-IR Data

Deep, high S/N CCD images of NGC 1316 in B, V, R, I and Hα filters were acquired from NED, and were observed with the Cerro Tololo Inter-American Observatory (CTIO) / University of Michigan Curtis Schmidt 0.6/0.9 m telescope (see Mackie & Fabbiano 1998 for details). The detector was a Thomson 1024 × 1024 CCD, with a pixel size of 19 μm and a spatial resolution of 1.83″ pixel^{-1}. These images were pre-processed, i.e. bias-subtracted, flat-fielded, co-added and exposure-corrected (Mackie & Fabbiano 1998). The sky background was estimated using the box method (Sahu et al. 1998) and was then subtracted from the respective passband image. The geometrically aligned, background-subtracted images were then used for the dust extinction study in the target galaxy. One of these cleaned B band images is shown in Figure 1, which reveals several shells, ridges and ripples around the main galaxy at larger radii; indicative of the mergers. With an objective to extend the study of dust extinction to cover other passbands, we acquired near-IR J, H and Ks band images of NGC 1316 from the archive of the Two Micron All Sky Survey (2MASS) observatory.

2.2 X-ray Data

Though the X-ray emission properties of NGC 1316 have already been reported using the observations from *Chandra* (Kim & Fabbiano 2003; Lanz et al. 2010), *XMM-Newton* (Isobe et al. 2006; Lanz et al. 2010), *SUZAKU* (Konami et al. 2010), *Einstein* (Fabbiano et al. 1992), as well as *ROSAT* (Kim et al. 1998), with an objective to examine the association of hot gas with dust and ionized gas in this merger remnant galaxy, we utilized high-resolution X-ray data of NGC 1316 from the archive associated with the *Chandra* observatory. NGC 1316 was observed by *Chandra* on 2001–04–17 (Obs. ID 2022) with the ACIS-S3 as the target for an effective exposure of 30.0 ks.

Standard tasks available within the *Chandra* Interactive Analysis of Observations (CIAO version 4.2.0) and the recent calibration files provided by the *Chandra* X-ray Center (CXC) (CALDB version 4.3.0) were employed for the analysis of X-ray data. These data sets were first filtered for the periods of high background emission using 3σ clipping of the 0.3–10.0 keV light curve extracted

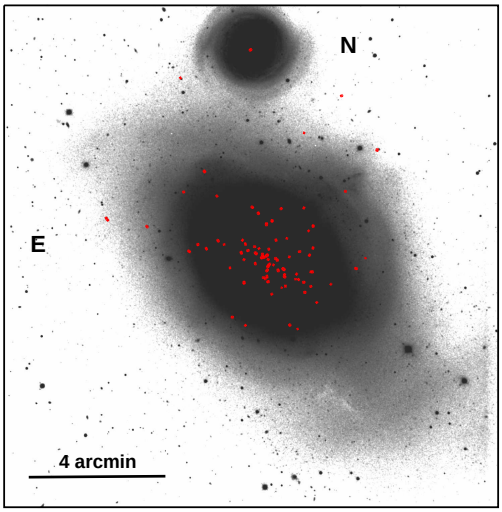

Fig. 1 A cleaned, background-subtracted B-band image of NGC 1316, overlaid on which are the *Chandra* X-ray point sources detected within the ACIS-S3 chip. This figure clearly reveals a set of shells and ripples as well as tails, signatures of the merger remnant.

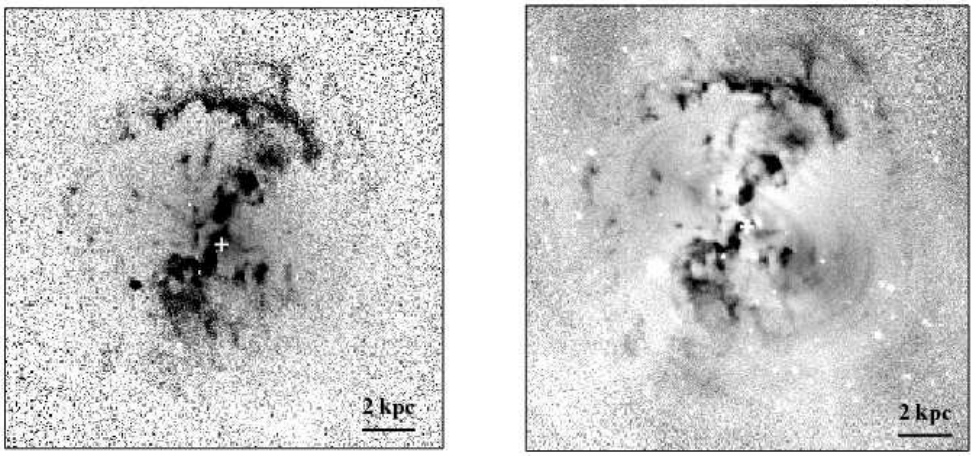

Fig. 2 The central $2.5' \times 2.5'$ region of NGC 1316. *Left panel*: the $(B - V)$ color index map; the darker shades delineate the regions that are occupied by dust and the plus indicates the position of the galaxy center as recognized by NED. *Right panel*: the B-band extinction map of NGC 1316.

from the chip with a binning of 260 s. This resulted in a net exposure time of 25.0 ks. For background subtraction, we correctly used the properly scaled blank sky background files provided by the CXC. The point sources recorded on chip S3 were detected using the *wavdetect* tool within CIAO adopting a detection threshold of 10^{-6} and scale parameter covering six steps between 1 and 32 pixels. This enabled us to detect a total of 86 discrete sources within the S3 chip. Out of the 86 detected sources, 80 were lying within the optical D_{25} region of NGC 1316 (Fig. 1).

3 RESULTS

3.1 Dust Properties

3.1.1 Dust extinction

Though NGC 1316 has been known to host dust features since its first detection by Schweizer (1980), the quantitative analysis of the extinction properties of dust in this galaxy is not available in the literature. To investigate the amount of dust extinction and its wavelength dependent nature, we need to know the spatial distribution and extent of the dust in the target galaxy. For this, we generated color index maps ($B-V$), ($B-R$), ($B-I$), etc. of NGC 1316 by comparing the light distribution in the geometrically aligned, seeing matched broadband images in different passbands.

Figure 2 (left panel) shows one such ($B-V$) color-index map of NGC 1316, where the darker shades represent the regions occupied by dust which are consistent with those reported by Schweizer (1980). This figure reveals a prominent dust lane along the optical minor axis of NGC 1316, which then takes an arc-like shape at about 6–7 kpc. In addition to these main features, several filament and clump like features are also evident in this figure.

Comparison of the light distribution in the extinguished part of the galaxies with that in the absence of dust allows us to investigate the extinction properties of dust and its wavelength-dependent nature (Brosch 1987; Patil et al. 2007). This can be done by deriving smooth models of the target galaxy in different passbands that are dust free. Here, the dust free models of NGC 1316 were generated by fitting ellipses to the isophotes in optical broadband images using the ISOPHOTE package within IRAF (see Patil et al. 2007 for details). The position angle, ellipticity and center coordinates were kept free during this fit until the signal reached 3σ of the background. Regions occupied by dust and foreground stars, as evident in the color index maps, were masked and ignored during the fit. The dust free models thus generated were used to quantify the wavelength-dependent nature of dust extinction, called the *extinction curve*, using the relation (Patil et al. 2007)

$$A_\lambda = -2.5 \log \left(\frac{I_{\lambda,\mathrm{obs}}}{I_{\lambda,\mathrm{model}}} \right),$$

where A_λ is the amount of total extinction in a particular passband (*B, V, R, I*), while $I_{\lambda,\mathrm{obs}}$ and $I_{\lambda,\mathrm{model}}$ are the observed (attenuated) and un-extinguished (modeled) light intensities in a given passband, respectively. One such extinction map derived for NGC 1316 is shown in Figure 2 (right panel). This figure confirms the unusual, intriguing and clumpy morphology of dust, as was evident in the ($B-V$) color index map of NGC 1316. From this figure it is apparent that in the inner part, dust appears in a well-defined lane oriented along its optical minor axis, which then takes an arc like form at about 6–7 kpc directed along the northeast direction. In addition to these main features, several knots, dust patches and clumps are also evident in this figure.

To investigate the quantitative properties of dust extinction and to examine how it depends on wavelength, total extinction values were measured in each passband by sliding a 5×5 box on the region occupied by dust. Numerical values of the local extinctions in each pass band (A_λ) were then used to derive the extinction values R_λ by fitting linear regressions between the total extinction A_λ and the selective extinction $E(B-V) = A_B - A_V$. The best-fitting slopes of these regressions, along with their associated uncertainties, were subsequently used to derive R_λ and hence the extinction curve. The extinction curve derived over the optical-to-near-IR region of the electromagnetic spectrum for the regions occupied by dust in the galaxy Fornax A (NGC 1316) is shown in Figure 3. From this figure it is clear that the dust extinction curve plotted between the measured values of $R_\lambda \left(= \frac{A_\lambda}{E(B-V)}\right)$ versus the inverse of the wavelength of their measurement varies linearly and closely follows the standard Galactic extinction law (Mathis et al. 1977), which is consistent with those derived for several other external galaxies (Goudfrooij et al. 1994; Sahu et al. 1996; Patil et al.

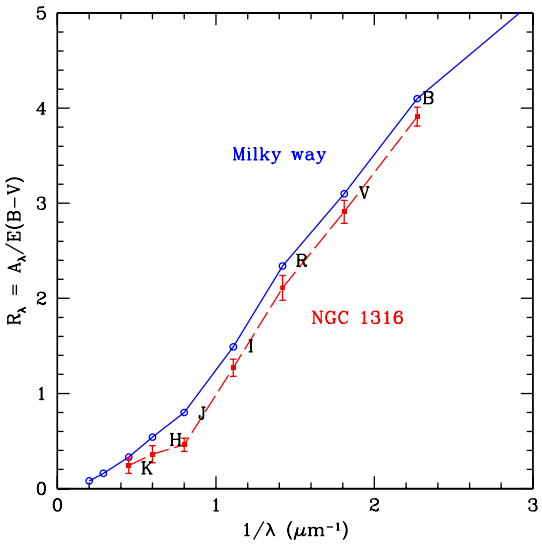

Fig. 3 Optical through near-IR extinction curve (*dashed line*) for NGC 1316 plotted as a function of the inverse of the wavelength. For comparison we also plot the standard Galactic extinction curve (*solid line*).

2001, 2002, 2003, 2007, 2009; Dewangan et al. 1999; Finkelman et al. 2012; Vagshette et al. 2012a). Relatively smaller values of R_λ in the case of NGC 1316 imply that the dust grains responsible for the extinction of optical and near-IR light are smaller than the canonical grains in the Milky Way, so that $\langle a \rangle < \langle a_{\rm Gal} \rangle$. This leads to $R_V = 2.91 \pm 0.12$ compared to 3.1 for the Milky Way.

3.1.2 Estimation of dust mass

The total extinction measured in the V band was used to quantify the dust content of NGC 1316. For this we integrated the dust column density $\Sigma_{\rm d}$ over the image area (A) occupied by the dust features in the V-band extinction map. Assuming that the chemical composition of the extragalactic dust is uniform throughout the galaxy and is identical to that in the Milky Way, we quantified the dust column density in NGC 1316. As the present study is limited to the range of optical to near-IR bands, we employed the simple two-component model, comprised of an adequate mixture of spherical silicate and graphite grains (Mathis et al. 1977). This model assumes there are uncoated refractory particles with a size distribution that follows a power law. The details of the dust estimation are described in Patil et al. (2007), but the dust mass can be estimated by integrating the dust column density over the area occupied by dust (A) using

$$M_{\rm d} = A \times \Sigma_{\rm d}\,.$$

For spherical grains of radius 'a' distributed with number density '$n_{\rm d}$' per unit volume in a cylindrical column of length '$l_{\rm d}$' and unit cross-sectional area along the line of sight, the reduction in intensity at a given wavelength in units of magnitude, i.e. the total extinction at wavelength λ, is given by

$$A_\lambda = 1.086\ \pi a^2 Q_{\rm ext}(a,\lambda) N_{\rm d}\,,$$

where $N_{\rm d} = \int n_{\rm d} dl$ is the dust column density and $Q_{\rm ext}(a,\lambda)$ is the extinction efficiency of the dust grain.

Instead of spherical grains of constant radius 'a,' if we assume the size distribution of $n(a) \propto a^{-3.5}$ (Mathis et al. 1977), then the expression for total extinction at wavelength λ becomes (see Kim et al. 1994),

$$A_\lambda = 1.086\ l_{\rm d} \int_{a_{\rm min}}^{a_{\rm max}} \pi a^2\ Q_{\rm ext}(a,\lambda)\ n(a)\, da = 1.086\ l_{\rm d} \int_{a_{\rm min}}^{a_{\rm max}} C_{\rm ext}(a,\lambda)\, n(a) da\,,$$

where $n(a)da$ represents the number of grains per unit volume along the line of sight with radii in the range a to $a + da$ (in cm^{-3}); $a_{\rm min}$ and $a_{\rm max}$ are the lower and upper cut-off in the distribution of grain size (in cm) respectively; $l_{\rm d}$ is the length of the dust column (in cm) and $C_{\rm ext}(a,\lambda) = \pi a^2\ Q_{\rm ext}(a,\lambda)$ is the total extinction cross-section at wavelength λ (in cm^2).

Using the value of $l_{\rm d}$, the dust column density (g cm^{-2}) can be expressed as,

$$\Sigma_{\rm d} = l_{\rm d} \times \int_{a_{\rm min}}^{a_{\rm max}} \frac{4}{3}\pi a^3 \rho_{\rm d}\ n(a)\, da\,.$$

This leads to the dust content of NGC 1316 being equal to 2.13$\times 10^5\, M_\odot$. For the average galactic extinction curve with $R_V = 3.1$, we assume $N_{\rm H}/A_V = 1.87 \times 10^{21}\,{\rm cm}^{-2}\,{\rm mag}^{-1}$ (Draine 2003). As this method assumes there is a screening effect from dust, it is insensitive to the dust component that is diffusely distributed throughout the galaxy. Thus, the dust mass estimated using optical extinction provides only the lower limit. The uncertainties involved due to the lower and upper cutoffs in the grain size may further worsen this estimate.

The dust content of NGC 1316 can alternatively be calculated using the IRAS flux densities at 100 μm and estimating the dust temperature by fitting a single temperature modified blackbody FIR SED over 60 – 500 μm of emissivity proportional to $\lambda^{-1.5}$ (Yun & Carilli 2002; Skibba et al. 2011). In the present case the dust temperature is found to be $T_{\rm d}$ = 26.8 K. Then we estimate the dust mass using the relation $M_{\rm d} = \frac{D^2 S_\nu}{\kappa_\nu B_\nu(T_{\rm d})}$, where κ_ν is the dust opacity, S_ν is the flux density, $B_\nu(T_{\rm d})$ is the Planck function for the dust grain temperature $T_{\rm d}$ and D is the distance to the galaxy in Mpc. Considering the value of dust emissivity given by Hildebrand (1983), emission flux at 100 μm, the dust mass in solar units is given by (Young et al. 1989),

$$M_{\rm d} = 4.78 S_{100\mu{\rm m}} D^2 \left[\exp\left(\frac{143.88}{T_{\rm dust}}\right) - 1\right],$$

and is found to be equal to 5.17$\times$10^6 $M_\odot$, an order of magnitude higher than that estimated using the optical extinction method. This discrepancy in the two estimates is due to the fact that the optical extinction method is insensitive to the component of dust that is intermixed, but IRAS can record this component. The estimate of dust temperature by a single-temperature gray body SED fit over 60–500 μm overestimates the dust grain temperature and hence underestimates the dust mass. Moreover, $\kappa \propto \lambda^{-1.5}$ assumes higher opacity at far-IR, and therefore leads to further underestimation of the dust content of the target galaxy. So the true dust content of NGC 1316 was estimated using the integrated MIPS data at 24 μm, 70 μm and 160 μm using the relation given by Muñoz-Mateos et al. (2009),

$$M_{\rm dust} = \frac{4\pi D^2}{1.616 \times 10^{-13}} \times \left(\frac{\langle \nu S_\nu \rangle_{70}}{\langle \nu S_\nu \rangle_{100}}\right)^{-1.801} \times C\ M_\odot,$$

where $C = (1.559\langle \nu S_\nu \rangle_{24} + 0.7686\langle \nu S_\nu \rangle_{70} + 1.347\langle \nu S_\nu \rangle_{160})$, D is the distance in Mpc and $\langle \nu S_\nu \rangle_{24}, \langle \nu S_\nu \rangle_{70}$ and $\langle \nu S_\nu \rangle_{160}$ are the MIPS flux densities at 24, 70 and 160 μm, respectively. The dust mass estimated using MIPS flux densities is found to be equal to 3.21$\times$10^7 $M_\odot$ and is in agreement with that reported by Lanz et al. (2010) and Draine et al. (2007), and is much higher than that estimated using the 100 μm flux densities of IRAS.

3.2 Association with Multiphase ISM

With the objective to examine the association of dust with ionized gas, we derived Hα + [N II] emission maps of NGC 1316 following the method discussed by Mackie & Fabbiano (1998). This was done by subtracting the properly scaled, sky-subtracted R-band continuum image from that of the emission-line image. The adopted scale factor was calculated by carrying out the least squares fit to the residuals of the field stars in the two frames. The resultant spatial distribution of the ionized gas within NGC 1316 is shown in Figure 4 (left panel) and closely matches that of the dust in the $(B-V)$ color map as well as the 3σ smoothed 0.3–3.0 keV X-ray emission map (Fig. 4 right panel). The arc of ionized gas in the Hα emission map appears more prominent compared to that in the dust extinction map.

3.3 X-ray Properties

3.3.1 Diffuse gas

The diffuse X-ray emission map derived for a galaxy is the best tool to delineate the morphology of hot gas. With an objective to examine the association of dust and Hα emitting ionized gas with the hot gas, we derived a 0.3–3.0 keV X-ray emission map for NGC 1316 from the analysis of *Chandra* observations, which is shown in Figure 4 (right panel). This figure represents the background subtracted, exposure corrected, point source removed, 3σ adaptively smoothed 0.3–3.0 keV *Chandra* image of NGC 1316, and is in agreement with that reported by Kim et al. (1998) using *ROSAT* data and by Kim & Fabbiano (2003) using *Chandra* data. Figure 4 clearly reveals the morphological similarities between the distribution of ionized gas and hot gas by exhibiting a strong correspondence between the two. For comparison we overplot contours of the Hα emitting gas on the X-ray image. Both of these morphologies closely follow that of the dust (Fig. 4 right panel), pointing towards a common origin for all three phases of the ISM. X-ray emission in the energy band 0.3–3.0 keV appears in a more extended form compared to that of the ionized gas, and shows a very disturbed structure along with filaments and patchy halos, which perhaps represent X-ray cavities. The orientation of the inner region of the dust lane appears to be slightly off that of the hot and warm gas.

Figure 5 illustrates the spatial correspondence between the different phases of ISM, including dust emission at 8 μm from the *Spitzer* data. The regions occupied by dust, mapped through the emission from polycyclic aromatic hydrocarbons observed at 8 μm using *Spitzer*, are found to coincide well with the X-ray emission in the central 7.5 kpc region.

To examine the global properties of hot gas in the target galaxy, we extracted a combined spectrum of the X-ray photons from within the optical D_{25} region of NGC 1316 that had the background subtracted and the point source removed. To avoid contribution from the nuclear source, we excluded the region around the central 20″. The spectrum was fitted following the standard χ^2 statistics within XSPEC version 12.6.0q with an absorbed single temperature MEKAL model. However, the fit exhibited residuals, particularly in the higher energy range. Therefore, to constrain the emission from the unresolved sources we added a power law component to it. Even after adding the power law component, the fit was not reliable and exhibited residuals. Then we tried with a double temperature plus a power law component (mekal + mekal + pl), which resulted in a relatively better fit with a χ^2 value close to 1.62 for 83 dof. During this fit, the hydrogen column density was fixed at the Galactic value of 2.40×10^{20} cm^{-2} (Dickey & Lockman 1990). The best fit resulted in $kT_{\rm cool} = 0.18 \pm 0.03$ keV, $kT_{\rm hot} = 0.62 \pm 0.02$ keV and the photon index being equal to $\Gamma = 0.45 \pm 0.10$.

With the goal of examining the temperature structure of the hot gas within NGC 1316, we performed spatially resolved spectral analysis of X-ray photons. For this we extracted 0.3–3.0 keV X-ray photons from eight different concentric annuli centered on the X-ray peak of NGC 1316. The width of each annulus was set such that we get roughly the same number of counts to validate the χ^2 statistics. The background spectrum was extracted from the exposure corrected blank sky

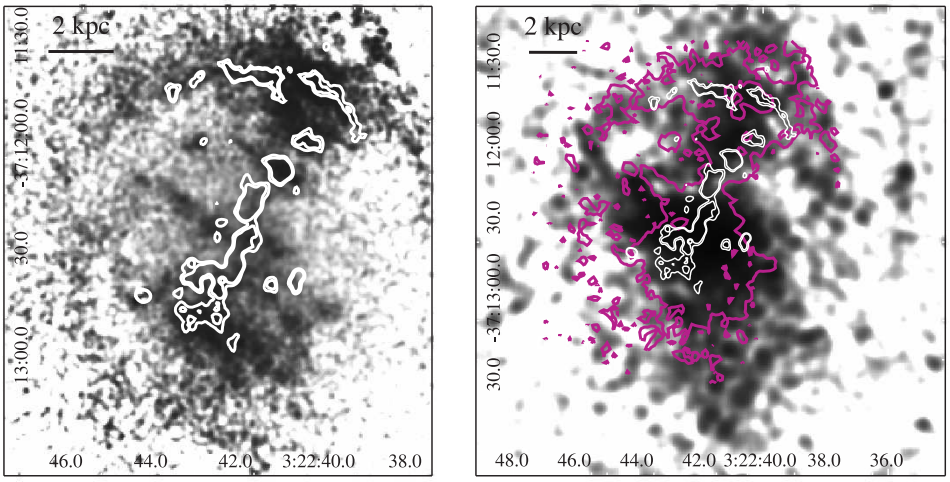

Fig. 4 *Left panel*: continuum subtracted Hα emission map, overlaid on which are the dust extinction contours (*white*). *Right panel*: 3σ smoothed 0.3–3.0 keV X-ray emission map, overlaid on which are the Hα emission contours (*pink*) and dust extinction contours (*white*).

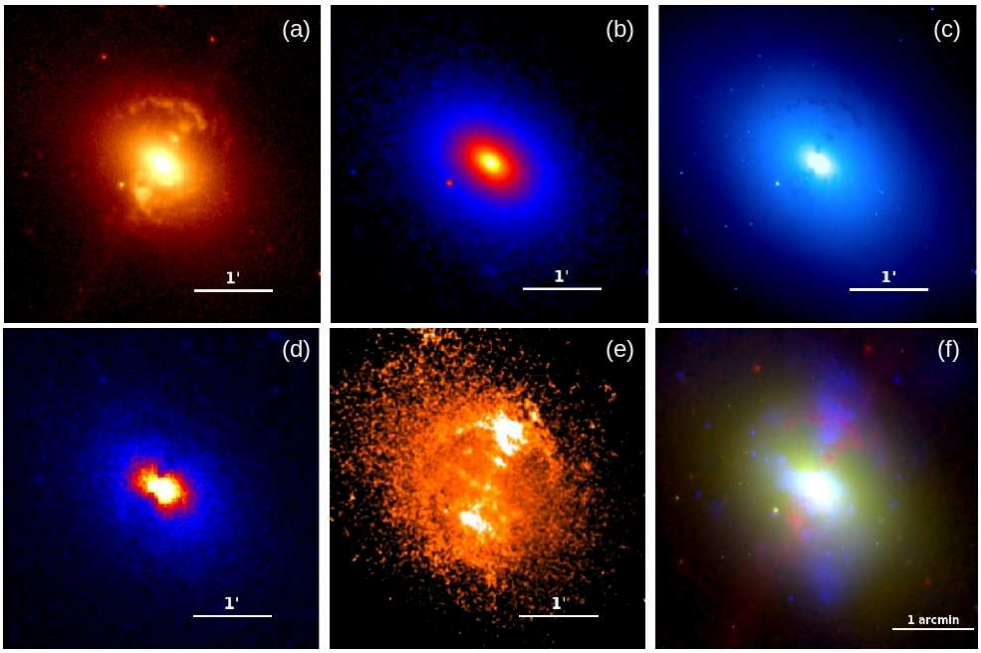

Fig. 5 The association with multiphase ISM in NGC 1316; (a) dust emission at 8 μm detected by *Spitzer*, (b) stellar light distribution mapped through the 2MASS K-band image, (c) stellar light distribution in the B-band, (d) near-UV GALEX image, (e) continuum subtracted Hα emission map, and (f) a tri-color map delineating multiphase association. The dust emission at 8 μm is represented in red, the blue band light distribution in green, and 0.3–3.0 keV hot gas in the blue.

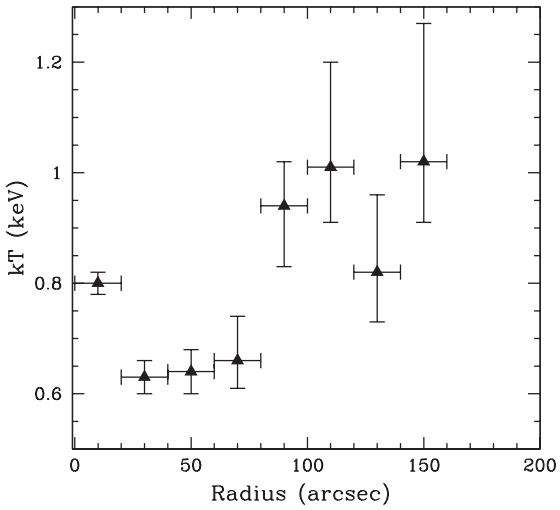

Fig. 6 Temperature profile of the hot gas distribution within NGC 1316 as a function radial distance. A positive temperature gradient can be confirmed from this figure.

frame provided by the CXC. Source spectra, background spectra, photon-weighted response files and photon-weighted files of the effective area were generated for each of the annuli using the CIAO tool *specextract*. Spectra extracted from each annulus were then fitted with a single-temperature thermal plasma model (*apec*) with a neutral hydrogen column density fixed at the Galactic value (Dickey & Lockman 1990). Temperature, metal abundance normalization, etc. were kept free during the fit. The resultant radial temperature profile derived for NGC 1316 is shown in Figure 6. From this profile it is evident that the X-ray photons distributed within NGC 1316 show a temperature structure in the sense that the temperature of the hot gas increases monotonically as a function of radial distance, like in the cooling flow of galaxies (Pandge et al. 2012, and references therein). A jump in the temperature profile is evident at about $1.2'$ and is perhaps linked to the dust absorption.

3.3.2 Discrete sources

As was discussed above, we detected 80 discrete X-ray sources within the optical D_{25} region of this galaxy. Discrete sources within a galaxy are thought to be linked to the star formation history and hence to the formation scenario of the host galaxy (Irwin et al. 2003; Colbert et al. 2004; Vagshette et al. 2012b). X-ray color plots of the X-ray binaries act as an efficient tool to investigate the characteristics of individual sources (Prestwich et al. 2003; Fabbiano 2006). The position of the source in this X-ray color plot clearly delineates its intrinsic nature and hence helps us to classify the sources into different types (Vagshette et al. 2012b). To investigate the X-ray characteristics of the resolved sources within NGC 1316, we derived an X-ray color plot for these sources. For this, we extracted background subtracted X-ray photons from individual sources in three different energy bands, namely soft (S, 0.3–1.0 keV), medium (M, 1.0–2.0 keV) and hard (H, 2.0–10.0 keV), using the task *dmextract* available within CIAO. Then, the hardness ratio of the individual source was estimated using the definitions $H21 = \frac{M-S}{S+M+H}$ and $H31 = \frac{H-M}{S+M+H}$ (Vagshette et al. 2012b). The plot between the X-ray hard (H31) versus soft (H21) color of all the sources is shown in Figure 7, from which it is apparent that the majority of the sources in this merger remnant galaxy are like normal $1.4\,M_{\odot}$ accreting neutron star low mass X-ray binaries (LMXBs) and are shown by the green

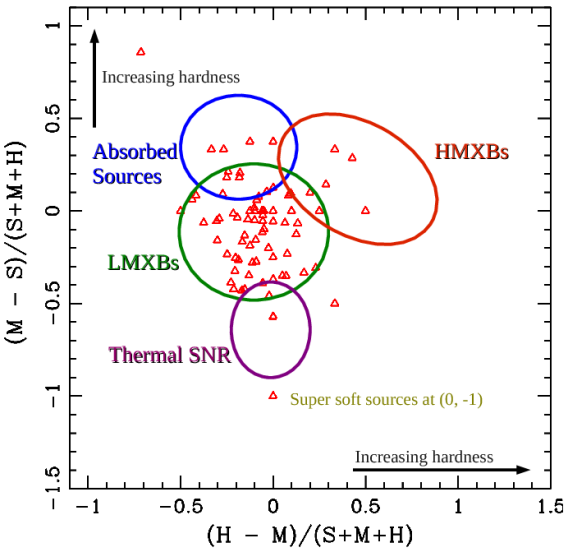

Fig. 7 X-ray color-color plot of the resolved sources plotted between X-ray hard color (H31) vs. soft color (H21). The structural properties of the different classes of sources are highlighted in the figure.

circle. Four of the remaining are high mass X-ray binaries (HMXBs), four are the heavily absorbed type, one is the super soft type and one is the heavily absorbed very hard source, perhaps the AGN. Although NGC 1316 is defined as a star forming galaxy, we found only one super soft source in this galaxy. In star forming galaxies, one expects a relatively larger population of super soft sources.

4 DISCUSSION

The origin of dust and gas in early-type galaxies is highly controversial. The internal origin of the dust in this class of galaxies assumes a contribution mainly from the asymptotic giant branch stars. Supernovae (SNe) have also been recognized as a potential candidate for the injection of dust and gas into the ISM (Dwek et al. 2007). The dust that is injected into the ISM is simultaneously processed by the forward and reverse shocks in the hot gas swept up by SNe and hence may undergo rapid erosion by sputtering (Nozawa et al. 2010). With the observed SNe rate in NGC 1316 and considering the two competitive processes of formation and simultaneous destruction of the grains, one can estimate the total content of dust that a galaxy may accumulate over its lifetime by solving the empirical relation (see Dewangan et al. 1999 for details),

$$\frac{\partial M_{\rm d}(t)}{\partial t} = \frac{\partial M_{\rm d,s}}{\partial t} - M_{\rm d}(t)\,\tau_{\rm d}^{-1},$$

where $\frac{\partial M_{\rm d}(t)}{\partial t}$ is the net dust accumulation rate; $\frac{\partial M_{\rm d,s}}{\partial t}$ is the rate at which dust is being injected by SNe and stellar winds; $\rm M_d(\mathit{t})$ is the amount of dust available at a given time t; and $\tau_{\rm d}^{-1}$ is the dust grain destruction rate. The life of the grains of radius a against sputtering due to electrons, hot protons and α-particles can be estimated by employing the relation given by Draine & Salpeter (1979) and in the present case it is found to be equal to $4.1\times 10^{-8}\,{\rm yr}^{-1}$. By assuming a gas-to-dust ratio of about ~ 100, the dust injection rate in NGC 1316 would be about $0.09\,M_{\odot}\,{\rm yr}^{-1}$. Therefore, the total build up (Fig. 8) of dust content in NGC 1316 over its life of $\sim$3 Gyr may be equal to $2.0 \times 10^{5}\,M_{\odot}$.

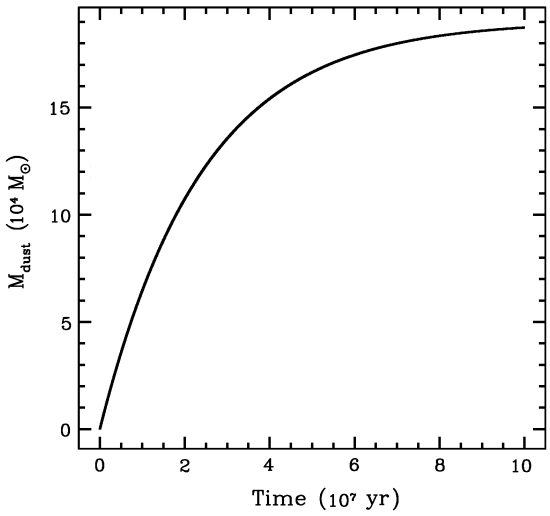

Fig. 8 Total build-up of the dust within NGC 1316 considering two competitive processes, i.e. injection versus destruction of the grains.

A comparison of the theoretically estimated mass of the dust with its true content derived using IR flux densities implies that the observed dust is far larger than what is expected to be accumulated by the galaxy over its lifetime. This discrepancy between the two estimates may be enhanced further if we include the amount of dust estimated using the observations at sub-mm wavelengths (Chini et al. 1995). Our estimate, based on the integrated MIPS flux densities, leads to a value of $3.21{\times}10^7\,M_\odot$ and is roughly two orders of magnitude larger than the amount of dust acquired internally by the galaxy. Thus, the internal supply of dust by the mass loss from evolved stars and SNe is insufficient to account for the observed amount of dust in this galaxy and hence favors its external origin through a merger-like event. Lanz et al. (2010) demonstrate its formation through the merging of late-type galaxies with a supply of $2-4\times10^9\,M_\odot$ of gas; enough to account for the observed values of dust and gas in this galaxy. There is other evidence that favors the formation of Fornax A through a merger-like event. The most important evidence is the presence of shells around the main optical part of the galaxy. Further evidence comes from the surprising similarity in the morphological appearance of the dust, warm gas and hot gas. Internally produced gas and dust must follow the stellar light distribution rather than preferred planes. Moreover, given the erosion of dust grains by sputtering, one expects anti-correlation between the internally produced dust and the ionized gas. However, there is growing evidence of a positive correlation between the two components, which strongly suggests the system formed through a merger-like process.

5 CONCLUSIONS

We present multiwavelength imagery of NGC 1316 with the objective of studying the dust content and other phases of the ISM, and its origin in the system. The results derived from this study are as follows.

– Color-index maps, as well as extinction maps, derived for NGC 1316 delineate the intricate morphology of the dust. This galaxy hosts a prominent dust lane oriented along the optical minor axis in the inner region, which then takes an arc-like shape at about 6 kpc. Apart from

these main features, several other knots/clumpy features are also evident in this galaxy. The dust emission maps derived using *Spitzer* observations at 8 μm exhibit even more complicated structure of the dust distribution.
– The extinction curve derived over the range of optical (B, V, R and I) to near-IR (J, H and Ks) bands for NGC 1316 closely follows the standard Galactic extinction law, implying that the properties of the dust grains in the merger remnant galaxy are identical to the canonical grains in the Milky Way.
– The dust content of NGC 1316 estimated using optical extinction is about $2.13 \times 10^5\, M_\odot$ and is an order of magnitude lower than that derived using the IRAS flux densities and two orders of magnitude lower than that using the integrated flux densities from MIPS at 24, 70 and 160 μm.
– The morphology of the hot gas derived from the analysis of high-resolution *Chandra* observations and ionized gas morphology mapped through Hα emission exhibits surprising similarities with the morphology of the dust, pointing towards a common origin of all the phases of ISM.
– The combined spectrum of the X-ray photons within the optical D_{25} region that had the point sources removed is well constrained by a double temperature together with a power law component, with the power-law component confirming the contribution from the unresolved population of sources.
– X-ray analysis enables us to detect a total of 80 discrete sources within D_{25}, the majority of which are normal LMXBs. X-ray color-color plots of the resolved sources exhibit the structural differences of the sources.
– Spatially resolved spectral analysis of the X-ray photons exhibited a temperature structure showing a positive gradient as a function of radial distance.

Acknowledgements The authors are grateful to the anonymous referee for their careful reading and encouraging comments on the manuscript that enabled us to improve the quality of the paper. This work is supported by UGC, New Delhi under the major research project F.No. (36-240/2008-SR). We acknowledge the use of the High Performance Computing Facility developed under the DST-FIST scheme sanction No. SR/FST/PSI-145. The use of the facilities at IUCAA, Pune is gratefully acknowledged. This work made use of data from the NASA/IPAC Extragalactic Database (NED), which is operated by the Jet Propulsion Laboratory, California Institute of Technology, under contract with the National Aeronautics and Space Administration, and data products from the *Chandra*, CTIO, GALEX, 2MASS, IRAS and MIPS archives.

References

Annibali, F., Bressan, A., Rampazzo, R., et al. 2010, A&A, 519, A40
Bertola, F. 1987, in Structure and Dynamics of Elliptical Galaxies, IAU Symposium, 127, eds. P. T. de Zeeuw, & S. D. Tremaine, 135
Brosch, N. 1987, MNRAS, 225, 257
Caon, N., Pastoriza, M., & Macchetto, D. 2001, Astrophysics and Space Science Supplement, 277, 409
Cappellari, M., Emsellem, E., Krajnović, D., et al. 2011, MNRAS, 416, 1680
Chini, R., Kruegel, E., Lemke, R., & Ward-Thompson, D. 1995, A&A, 295, 317
Colbert, E. J. M., Heckman, T. M., Ptak, A. F., Strickland, D. K., & Weaver, K. A. 2004, ApJ, 602, 231
Dewangan, G. C., Singh, K. P., & Bhat, P. N. 1999, AJ, 118, 785
Dickey, J. M., & Lockman, F. J. 1990, ARA&A, 28, 215
Draine, B. T. 2003, ARA&A, 41, 241
Draine, B. T., Dale, D. A., Bendo, G., et al. 2007, ApJ, 663, 866
Draine, B. T., & Salpeter, E. E. 1979, ApJ, 231, 438
Dwek, E., Galliano, F., & Jones, A. P. 2007, ApJ, 662, 927
Ekers, R. D., Goss, W. M., Wellington, K. J., et al. 1983, A&A, 127, 361

Fabbiano, G. 2006, ARA&A, 44, 323
Fabbiano, G., Kim, D.-W., & Trinchieri, G. 1992, ApJS, 80, 531
Feigelson, E. D., Laurent-Muehleisen, S. A., Kollgaard, R. I., & Fomalont, E. B. 1995, ApJ, 449, L149
Finkelman, I., Brosch, N., Funes, J. G., et al. 2012, MNRAS, 422, 1384
Finkelman, I., Brosch, N., Kniazev, A. Y., et al. 2010, MNRAS, 409, 727
Goudfrooij, P., Hansen, L., Jorgensen, H. E., & Norgaard-Nielsen, H. U. 1994, A&AS, 105, 341
Goudfrooij, P., Alonso, M. V., Maraston, C., & Minniti, D. 2001, MNRAS, 328, 237
Goudfrooij, P., Gilmore, D., Whitmore, B. C., & Schweizer, F. 2004, ApJ, 613, L121
Hildebrand, R. H. 1983, QJRAS, 24, 267
Irwin, J. A., Athey, A. E., & Bregman, J. N. 2003, ApJ, 587, 356
Isobe, N., Makishima, K., Tashiro, M., et al. 2006, ApJ, 645, 256
Kim, S.-H., Martin, P. G., & Hendry, P. D. 1994, ApJ, 422, 164
Kim, D.-W., Fabbiano, G., & Mackie, G. 1998, ApJ, 497, 699
Kim, D.-W., & Fabbiano, G. 2003, ApJ, 586, 826
Konami, S., Matsushita, K., Nagino, R., et al. 2010, PASJ, 62, 1435
Kormendy, J., & Djorgovski, S. 1989, ARA&A, 27, 235
Lanz, L., Jones, C., Forman, W. R., et al. 2010, ApJ, 721, 1702
Mackie, G., & Fabbiano, G. 1998, AJ, 115, 514
Malin, D. F., Quinn, P. J., & Graham, J. A. 1983, ApJ, 272, L5
Mathis, J. S., Rumpl, W., & Nordsieck, K. H. 1977, ApJ, 217, 425
Muñoz-Mateos, J. C., Gil de Paz, A., Boissier, S., et al. 2009, ApJ, 701, 1965
Nozawa, S., Kohyama, Y., & Itoh, N. 2010, Phys. Rev. D, 81, 083007
Pandge, M. B., Vagshette, N. D., David, L. P., & Patil, M. K. 2012, MNRAS, 421, 808
Patil, M. K., Pandey, S. K., Kembhavi, A. K., & Singh, M. 2001, Bulletin of the Astronomical Society of India, 29, 453
Patil, M. K., Sahu, D. K., Pandey, S. K., et al. 2002, Bulletin of the Astronomical Society of India, 30, 759
Patil, M. K., Pandey, S. K., Sahu, D. K., & Kembhavi, A. K. 2003, Multi-wavelength Study of Dust Properties in Early-type Galaxies, in Astrophysics of Dust, Estes Park, Colorado, May 26 - 30, 2003. ed. A. N. Witt
Patil, M. K., Pandey, S. K., Sahu, D. K., & Kembhavi, A. 2007, A&A, 461, 103
Patil, M. K., Pandey, S. K., Kembhavi, A., & Sahu, D. K. 2009, arXiv:1202.2434
Prestwich, A. H., Irwin, J. A., Kilgard, R. E., et al. 2003, ApJ, 595, 719
Rampazzo, R., Annibali, F., Bressan, A., et al. 2005, A&A, 433, 497
Sahu, D. K., Pandey, S. K., Chakraborty, D. K., Kembhavi, A., & Mohan, V. 1996, A&A, 314, 721
Sahu, D. K., Pandey, S. K., & Kembhavi, A. 1998, A&A, 333, 803
Sarzi, M., Falcón-Barroso, J., Davies, R. L., et al. 2006, MNRAS, 366, 1151
Schweizer, F. 1980, ApJ, 237, 303
Schweizer, F., & Seitzer, P. 1988, ApJ, 328, 88
Skibba, R. A., Engelbracht, C. W., Dale, D., et al. 2011, ApJ, 738, 89
Terlevich, A. I., & Forbes, D. A. 2002, MNRAS, 330, 547
Vagshette, N. D., Pandge, M. B., Pandey, S. K., & Patil, M. K. 2012a, New Astron., 17, 524
Vagshette, N. D., Pandge, M. B., & Patil, M. K. 2012b, arXiv: 1205.6057
Young, J. S., Xie, S., Kenney, J. D. P., & Rice, W. L. 1989, ApJS, 70, 699
Yun, M. S., & Carilli, C. L. 2002, ApJ, 568, 88